IIARD International Journal of Geography & Environmental Management
Vol. 10 No. 12 2024 E-ISSN 2504-8821 P-ISSN 2695-1878 www.iiardjournals.org Online Version

Identification of Groundwater Potential Zones in Hard Rock Terrain of Osun State, Nigeria: Insights from Knowledge-Based (AHP) and Data-Driven (FR) Models

Joshua Oluwasanmi Owoseni
Federal University of Technology Akure, School of Earth and Mineral Sciences, Nigeria.
E-mail: joowoseni@futa.edu.ng; jo.owoseni@gmail.com
ORCID: 0000-0001-9992-4569
DOI: 10.56201/ijgem.v10.no12.2024.pg33.57

ABSTRACT
The uncertainties associated with groundwater prospecting in the hard rock terrains can be daunting due to erratic nature of aquifers. However, the exploration time and cost can be reduced drastically by narrowing down search areas for geophysical exploration through implementation of a preliminary GIS-based groundwater productivity mapping. This is the focus of the current study across the hard rock terrain of Osun State, Nigeria, with a view to providing a groundwater potential map for land use planning and groundwater resource development. Knowledge-based (AHP) and data-driven (FR) techniques were adopted for allocating weightages to ten applicable groundwater conditioning factors which form the thematic layers. The themes are lithology, rainfall, soil, slope, lineament density, land use, altitude, topographic wetness index, drainage density, and drainage proximity. The weighted linear combination approach was used to aggregate the themes by an overlay analysis in GIS environment. The receiver operating system (ROC) curve was used to validate the groundwater potential maps produced, using borehole yield data. The AHP model results show the order of influence of the conditioning factors as, lithology (37.4%), rainfall (11%), altitude (9.8%), soil (9.6%), lineament density (9.0%), land use (6.4%), drainage density (6.4%), and proximity to drainage (4.7%), slope (3.9%), and topographic wetness index (1.9%). The area under curve (AUC) values of 0.731 and 0.717 were obtained and they translate to prediction accuracies of 73.1% and 71.7% for AHP and FR models respectively. The groundwater potential maps can aid sustainable groundwater resources development in the study area.
Keywords *Analytic hierarchy process, Remote sensing, Frequency ratio, Water security, GIS, Groundwater potential zone.*

1. INTRODUCTION

Groundwater is the major source of available freshwater on the planet earth. However, its occurrence and spatiotemporal distribution is often dependent on several related factors, some of which are, geology, geomorphology, lineaments, drainage system, climate change, rainfall, land use and land cover. The alarming impact of climate change and anthropogenic activities on the availability of groundwater resources in different parts of the world has been reported in the literature (Earman and Dettinger, 2011; Wu et al, 2020; Hughes et al., 2021; Yifru, et al., 2021; Swain et al., 2022). Water security is fast becoming a key issue of concerns globally, featuring prominently in the Millennium Development Goals (MDGs) and Sustainable Development Goals (SDGs). The ever-growing population in Nigeria is increasingly dependent on groundwater resources for domestic and industrial uses. The phenomenal population

growth, increasing industrialization, urbanization, and competition for economic development across the country, are all aggravating demand for and stress on
available groundwater resources (Foster et al., 1998; Nwankwoala, 2014). About 50% of the country's landmass is underlain by crystalline Basement complex rocks where groundwater occurrence is highly dependent on thickness of weathered overburden material and lineament (fractures) density in fresh underlying bedrock. Hence, the yield from boreholes in hard rock terrains of the study area are not expected to be so much except in places with deep weathering and high lineament density which favour large scale groundwater development (Akinwumiju and Olorunfemi, 2016).

The advantages of groundwater over surface water cannot be overemphasized in a low economy such as, Nigeria. The cost of groundwater development and usage is cheaper than that of surface water. Hence, groundwater development is common for both rural and urban water supplies across the country. Its availability in both wet and dry seasons is an added benefit over surface and rain-harvested water. Besides, groundwater possesses better quality than surface water, and does not require sophisticated treatment for drinking purpose. Nevertheless, the uncertainties associated with groundwater prospecting in the crystalline basement terrains can be intimidating due to unpredictable nature of aquifers. Various factors, namely, geology, soil media (texture and thickness), lineament density, and rainfall distribution, play major roles in groundwater spatiotemporal distribution (Offodile, 1992; Akinluyi, 2013; Fashae et al., 2014; Aluko and Igwe, 2017; Abdulazeez & Naisa, 2018; Oyedele, 2019). In Osun State, rainfall is the main source of groundwater recharge, and effective rainfall last for barely eight months (March - October) per year. The area is underlain by crystalline basement rocks whose aquifer characteristics depend on their degree of weathering and fracturing. Hence, groundwater storage capacity varies based on factors such as, the thickness of weathered zone, lineament density, effective porosity and permeability. The population growth rate and density for the study area were put at 3.25% and 379 persons/sq. km (NPC, 2009). The ever-growing population is increasingly dependent on groundwater resources for domestic, industrial, and other purposes. Water security in the area requires adoption of appropriate groundwater prospecting techniques in view of the hard rock terrain.

Various techniques, namely, geophysical, geospatial, hydrogeological, and geochemical methods have been adopted over the years in groundwater exploration (Adiat et al., 2013; Mogaji and Lim, 2013; Afshar et al., 2015; Day-Lewis et al, 2017; Al-Djazouli et al., 2019; Diaz-Alcaide and Martinez-Santos, 2019; Olorunfemi, et al., 2020). However, in the last few decades, GIS-based multi-criteria decision analysis (MCDA) and remote sensing techniques for groundwater potential mapping have been extensively reported globally (Chowdhury et al., 2009; Kaliraj et al., 2014; Pinto et al., 2017; Kumar and Krishna, 2018; Al-Djazouli et al., 2020). The benefits of the geospatial technologies include reliability, cost-effectiveness, and simplicity (Abijith et al, 2020). Therefore, the current study applies a knowledge-based, Analytical Hierarchical Process (AHP) model (Saaty, 1980), and a data-driven, Frequency Ratio (FR) model for identification of potential groundwater recharge zones in Osun State, Nigeria. The two approaches simplify decision-making process and have been reportedly successful all over the world (Davoodi et al., 2013; Al-Abadi, 2015; Razandi et al., 2015; Saha, 2017; Abrams et al., 2018; Andualem & Demeke, 2019; Abijith et al., 2020; Arshad et al., 2020; Hamdani and Baali, 2020). The aim of the current study was to conduct a GIS-based

groundwater productivity mapping in hard rock terrain of Osun State, Nigeria, using knowledge-based analytic hierarchy process and data-driven frequency ratio models. This is with a view to narrowing down the search areas for geophysical investigation, thereby saving some time and cost without compromising quality of results.
The resulting groundwater potential maps will be veritable tools in land use planning and groundwater resources development in the state. The specific objectives for realizing the aim of the study include, allocation of appropriate weights to adopted groundwater conditioning criteria, generation of thematic layers, integration of thematic layers by overlay analysis, and validation of groundwater potential maps.

1.1 Study area

The study area is crystalline basement rock terrain, situated within latitudes 6°55′00″ N and 8°05′00″ N, and longitude 4°00′00″ E and 5°05′00″ E, covering an area of 9,026 km^2 in the southwestern part of Nigeria (Figure 1). The altitude varies between 66 and 768 meters above the mean sea level. The climate is tropical, and characterized by distinct wet and dry seasons which favour the formation of residual reddish brown lateritic soils. The temperature ranges between 21° C (around August) and 32° C (around February). Relative humidity in the area varies from 70% to 90% around January and July respectively. Annual rainfall fluctuates between 1,313 and 1,961 millimetres. The projected population of Osun State in 2030 have been put at 7,363,464 at 3.25% growth rate. Figure 2 shows a population sprawl for the area between 2010 and 2030 (NPC, 2009).

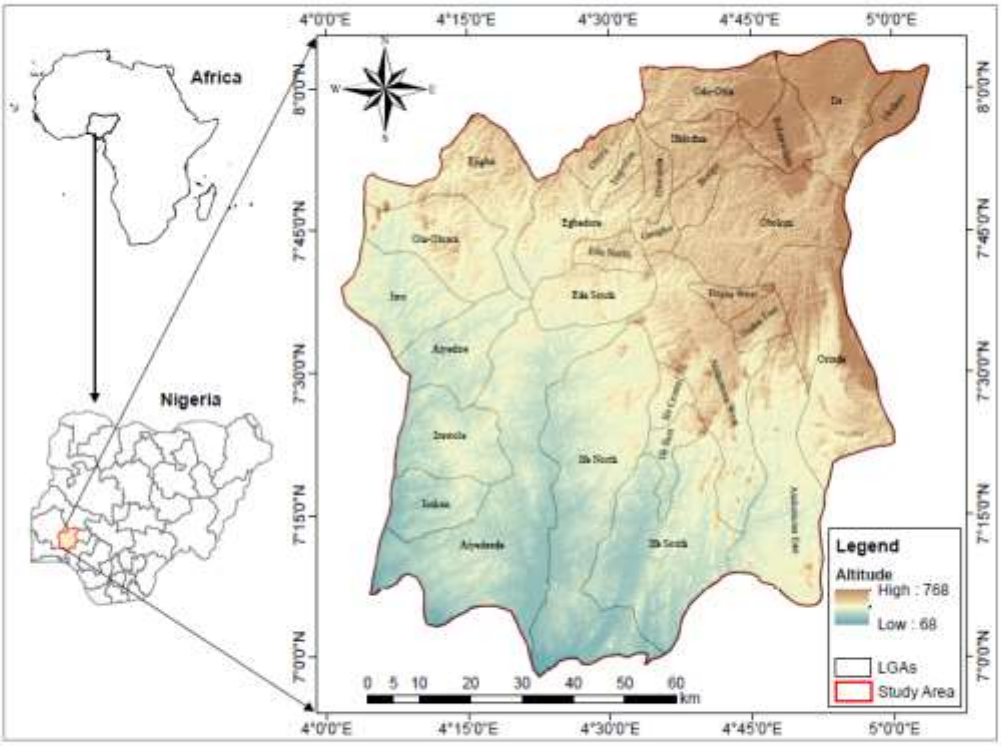

Fig. 1 Location map of the study area

Agriculture is the major economic activity in the study area. The region is known for cultivation of cash crops like cocoa, oil palm, kola nut and cotton. Common food crops include cassava, rice, maize, plantain, banana and yam. Other important economic activities in the area include commerce, woodwork, pottery, craftsmanship, blacksmithing, herbal medicine preparation, textile dying and weaving. There are gold deposits around Ilesha where mining activities are ongoing. Ilesha also hosts a number of publicly and privately owned educational institutions, industries, banks, and hotels. Osogbo, the State capital, is known for tourism, and is fondly referred to as the home of traditional textile dyeing.

1.2 Geological setting

The regional geology of the study area comprises basically the Precambrian Basement Complex rocks, namely, minor intrusive rocks, older granites, schist belts, and migmatite-gneiss-quartzite complex. The local lithological units underlying the study area are the older granites (granitoids), schist belts (meta-sediments) and migmatite-gneiss-quartzite complex (Adekoya et al., 2003; Elueze, 2002). Occurrence of groundwater is largely dependent on thickness of weathered overburden layer, and degree of fracturing of the underlying fresh crystalline rocks. Structural features prominent on the migmatite-gneiss-quartzite complex include veins, veinlets, foliations, joints, faults and folds. According to Olorunfemi et al. (1999), the foliations trend NNW-SSE and NNE-SSW, and the fissure zones trend N-S.

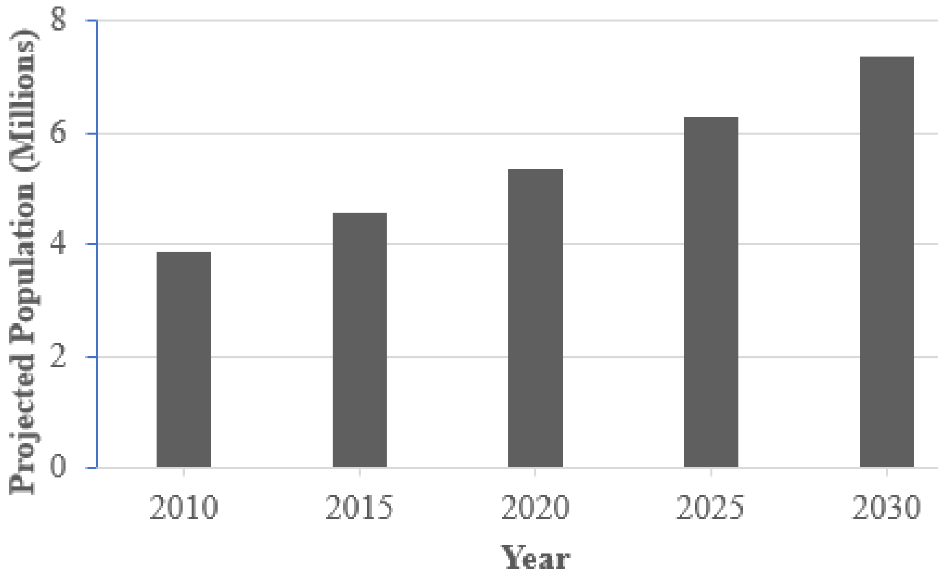

Fig. 2 Population projection for Osun State at 3.25% growth rate (National Population Commission, 2009).

2. MATERIALS AND METHODS

The various datasets used for groundwater potential mapping in the study, and their sources, are presented in Table 1. Two tiles of Shuttle Radar Tomography Mission (SRTM) Digital Elevation Model (DEM) at one arc second (30 meters) resolution were downloaded from the United State Geological Survey (USGS, 2004) website in April, 2017, for producing the desired altitude, slope angle, topographic wetness index, and drainage density maps. Landsat 8 OL1 imagery covering the region was downloaded from USGS website in November, 2022 for generating land use map. The geological, and lineament maps depicting the surface outcrops, sub-surface rocks and linear structures in the rocks across the area were adapted from published works (NGSA, 2006a; NGSA, 2006b). Soil map for the area was acquired from the

Federal Department of Agricultural Land Resources. Groundwater potential mapping in the present study followed a 7-step procedural method organized as a flowchart (Figure 3) and described below.

2.1 Selection of appropriate evaluation criteria

The significance of selecting appropriate criteria controlling groundwater occurrence and distribution in an area cannot be overemphasized. Hence, ten groundwater conditioning factors were carefully selected for evaluating groundwater potential in the current study through combined expert knowledge, and literature review. The features include, lithology, rainfall, soil media, slope angle, lineament density, land use/cover, altitude, topographic wetness index, drainage density, and drainage proximity.

Table 1 Data used and their sources

Data	Year	Resolution	Relevance	Source
SRTM DEM imagery	2004	30m	To generate altitude, slope, TWI, and drainage maps	USGS website
Landsat 8 imagery	2020	30m	To generate land use/land cover map	USGS website
Lineament map	2006	1:2,000,000	To extract the faults in the study area	NGSA
Geological map	2006	1:250,000	To extract the geological map of the area	NGSA
Soil map	1990	1:1,000,000	To extract the soil types for the study area	FDALR

USGS (United State Geological Survey); NGSA (Nigerian Geological Survey Agency); FDALR (Federal Department of Agricultural Land Resources); TWI (Topographic Wetness Index)

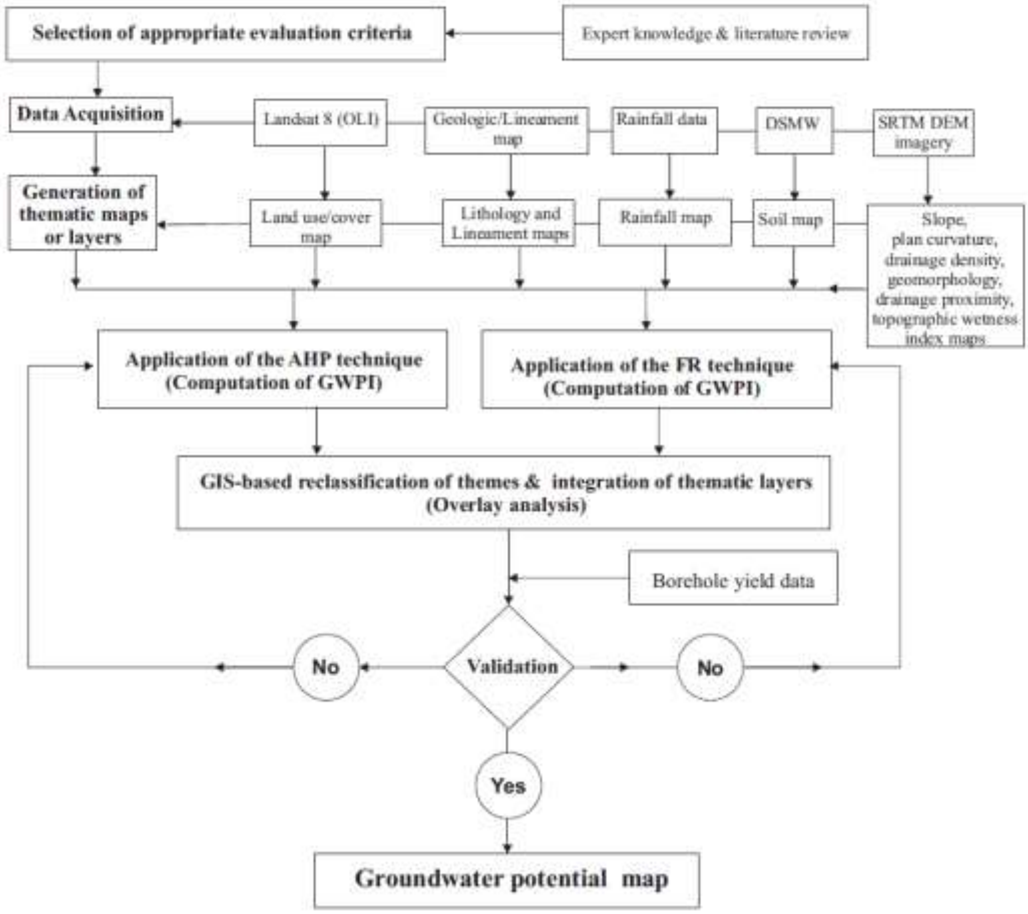

Fig. 3 Flowchart for Groundwater prospecting in the study area

2.2 Generation of thematic layers

ArcGIS 10.2 was used for geospatial data processing and analysis to generate thematic map layers representing the ten selected groundwater conditioning parameters for groundwater potential mapping. Scanned geological, lineament, and soil maps of the area were georeferenced, digitized, rasterized, and classified using the spatial analyst tool in ArcMap, to obtain the required lithology, lineament, and soil thematic layers. The line density tool was used to generate a lineament density map from the lineament map according to equation (1).

$$LD = \sum_{i=1}^{n} Li/A\,(km/km^2) \qquad \text{.. (1)}$$

where *LD* is lineament density, *Li* is the total length of all lineaments in km, and *A* is the area in km^2.

The Inverse Distance Weighted (IDW) interpolation technique, a common technique for interpolating raster surfaces from point data, was used to rasterize imported rainfall data in ArcMap. The raster map was then classified to generate the required rainfall thematic layer. Two tiles of SRTM digital elevation model (DEM) of the area were mosaicked, and processed using the spatial analyst tool to produce the altitude, slope, and topographic wetness index (TWI), and drainage maps. The TWI is defined according to equation (2).

$$TWI = \ln\left(\frac{S_a}{tan\theta}\right) \quad \text{.. (2)}$$

where, *TWI* is topographic wetness index, S_a is the cumulative upslope area draining through a point per unit contour length, and θ is gradient in degree.

The drainage map was further processed using the line density and the Euclidean distance tools in ArcMap to generate the drainage density, according to equation (3), and drainage proximity maps respectively. The Landsat 8 OL1 imagery was processed and classified by supervised classification using the maximum likelihood technique to generate the desired land use/cover thematic map.

$$DD = \sum_{i=1}^{n} Si/A \, (km/km^2) \quad \text{.. (3)}$$

where, *DD* is drainage density, *Si* is the total length of all streams in km, and *A* is the area in km^2.

2.3 Analytic hierarchical process (AHP) model

2.3.1 Assignment and normalization of weights, and consistency check

The Analytic Hierarchy Process (AHP) which was first introduced by Saaty (1980), is a popular tool which has been used successfully and well reported in the literature on groundwater potential mapping (Fashae et al., 2014; Rahmati et al., 2016; Arulbalaji et al., 2019; Roy et al., 2020; Tolche, 2020; Abijith et al., 2020; Arshad et al., 2020; Hamdani and Baali, 2020). For the purpose of determining the normalized weight of each of the selected groundwater productivity criteria, an appropriate weight was assigned to each criterion using the Saaty's 9-point scale of relative importance (Table 2), based on experts' knowledge, and the pairwise comparison matrix was computed using Microsoft Excel version 2016. The assigned weights were normalized to reduce any associated subjectivity using AHP, and eigenvector approach. The consistency in weight allocation to produce the comparison matrix was verified by computing Consistency Ratio (CR) which involved three steps, namely,
(i) computation of eigenvalue using eigenvector technique which normalized the assigned weights, (ii) calculation of Consistency Index (CI) according to equation (4), (iii) computation of Consistency Ratio (CR) following equation (5). Since ten conditioning factors were used, the value of 1.49 was adopted as the Random Index (RI) as suggested by Saaty (Table 3). The classes under each criterion were ranked on a groundwater potentiality scale, namely, 1 (very low), 3 (low), 5 (moderate), and 7 (high) based on groundwater occurrence, following Al-Djazouli *et al.* (2020).

$$CI = \frac{\lambda_{max} - n}{n-1} \quad \text{........................ (4)}$$

where, λ_{max} is the maximal eigenvalue for the pair-wise comparison matrix and *n* is the dimension of the matrix (number of criteria used for groundwater potential evaluation).

$$CR = \frac{CI}{RI} \quad \text{........................ (5)}$$

where, CR is the consistency ratio, CI is the consistency index, and RI is the random index.

For the weights assigned in computing the pair-wise comparison matrix to be considered reasonably consistent, consistency check was conducted. The matrix and resulting normalized weights computed were adopted because the value of the consistency ratio (CR) obtained was within the acceptable range, namely, CR ≤ 0.1 (Saaty, 1980). The normalized weights for the conditioning factors were used for overlay analysis in ArcMap to generate a groundwater potential map for the study area.

Table 2 Saaty's scale of relative importance (Saaty, 1980).

Scale	1/9	1/7	1/5	1/3	1	3	5	7	9
Level of importance	Extremely less important	Very strongly less important	Strongly less important	Moderately less important	Equally important	Moderately more important	Strongly more important	Very strongly more important	Extremely more important

Table 3 Saaty's random index (RI) for different numbers of criteria (n)

Number of criteria, *n*	2	3	4	5	6	7	8	9	10
Random Index, RI	0	0.58	0.90	1.12	1.24	1.32	1.41	1.45	1.49

2.3.2 Overlay analysis

The weighted linear combination (WLC) technique was implemented for integrating the ten thematic layers in ArcMap 10.2 in order to generate a groundwater potential map for the study area. The groundwater potential index (GWPI) was computed using the raster calculator tool in ArcMap according to equation (6) (Malczewski, 1991).

$$GWPI_{AHP} = LG_{Wi}LG_{wj} + RN_{Wi}RN_{wj} + SM_{Wi}SM_{wj} + SA_{Wi}SA_{wj} + LD_{Wi}LD_{wj} + LU_{Wi}LU_{wj} + AT_{Wi}AT_{wj} + TW_{Wi}TW_{wj} + DD_{Wi}DD_{wj} + DP_{Wi}DP_{wj} \quad \text{.......} \ldots \ldots \ldots \ldots (6)$$

where, $GWPI_{AHP}$ is groundwater potential index using AHP model, LG is lithology, RN is rainfall, SM is soil media, SA is slope angle, LD is lineament density, LU is land use/cover, AT is altitude, TW is topographic wetness index, DD is drainage density, DP is drainage proximity, subscript *wi* is the normalized weight of each thematic layer, and subscript *wj* is the normalized weight of each sub-class within respective thematic layers.

2.4 Frequency ratio (FR) model

The Frequency ratio (FR) model is a data-driven bivariate statistical approach commonly employed in computing the probabilistic spatial relationship between dependent (groundwater well locations) and independent (groundwater potential map) variables (Oh et al., 2011). The success of its usage in groundwater potential mapping has been reported in the literature (Razandi et al., 2015; Arshad et al., 2020). The value of FR was computed for individual sub-class in each thematic layer representing the ten groundwater conditioning factors according to equation (7).

$$FR = \frac{\%\,Well\ pixels}{\%\,Class\ pixels} = \frac{C_w/T_w}{C_p/T_p} \quad \ldots\ldots\ldots\ldots\ldots\ldots\ldots\ldots\ldots\ldots (7)$$

where FR is the frequency ratio, C_w is the number of well pixels in each sub-class, T_w is the total number of well pixels in the study area, C_p is the number of pixels in each sub-class, and T_p is the total number of pixels in the study area. The groundwater potential index for the FR model was computed using equation (8).

$$GWPI_{FR} = \sum_{i=1}^{i=n} FR_i \qquad \text{.................................. (8)}$$

where, $GWPI_{FR}$ is the groundwater potential index for FR model, and FR_i is the final weight for the FR model.

2.5 Validation of groundwater potential map

The significance of validation in scientific model application cannot be overemphasized (Nampak et al., 2014). Validation helps to determine the degree of accuracy of model results (Jaafari et al., 2014). Groundwater yield data which reflects groundwater occurrence was used to validate the groundwater potential maps generated in the current study. The receiver operating characteristics (ROC) curve which gives area under curve (AUC) value indicating the accuracy of model results is a commonly used validation technique in groundwater potential evaluation (Razandi et al., 2015; Abijith et al., 2020; Arshad et al., 2020). The ROC curves for AHP-derived and FR-produced groundwater potential models were generated using Spatial Data Modeller for ArcGIS (ArcSDM 10) in ArcMap 10.2. The prediction accuracy of the AHP and FR models indicated by the respective AUC values was interpreted using the classification scheme of Yesilnacar (2005), namely, excellent (0.9 – 1.0), very good (0.8 – 0.9), good (0.7 – 0.8), satisfactory (0.6 – 0.7), and unsatisfactory (0.5 – 0.6).

3. RESULTS AND DISCUSSION

The various thematic maps of groundwater conditioning factors generated, reclassified and ranked according to groundwater potentiality are presented and discussed below. The results gotten from the application of analytic hierarchical process (AHP) and frequency ratio (FR) models for delineating groundwater potential zones in the study area, are also included.

3.1 Thematic layers

3.1.1 Lithology

The significance of lithology in groundwater occurrence and distribution cannot be overemphasized. The higher the hydraulic conductivity of any lithologic unit or its weathering product, the higher the rate of infiltration and flow of groundwater through it, and the higher its potential for groundwater storage. The hydraulic properties (effective porosity and permeability) of the crystalline igneous and metamorphic rocks are key factors influencing spatial distribution of groundwater in the study area. Hence, the older granites can only serve as groundwater reservoirs when weathered and/or fractured. The lithologic units of the study area were ranked 1 (migmatite gneiss), 2 (granitoids), 3 (meta-sediments), and 4 (quartzites), corresponding to very low, low, moderate, and high groundwater potentialities respectively (Figure 4). These corresponded to 3538.04 km^2 (38.55%), 2339.97 km^2 (25.49%), 2363.52 km^2 (25.75%) and 936.76 km^2 (10.21%) of the study area respectively (Table 4).

3.1.2 Rainfall

Rainfall is an important evaluation criterion for determining potential groundwater recharge zones because the storage potential of any aquifer is dependent on rates of groundwater recharge and discharge. The quantity of rainfall infiltrating to recharge groundwater system depends on duration and intensity of rainfall. In the study area, rainfall is the major source of groundwater recharge with annual estimates ranging from 1,313 mm/year to 1,961 mm/year (Figure 5). Rainfall point data for the area was interpolated using IDW tool in ArcGIS 10.2 to produce a raster map showing spatial distribution of rainfall for the area.

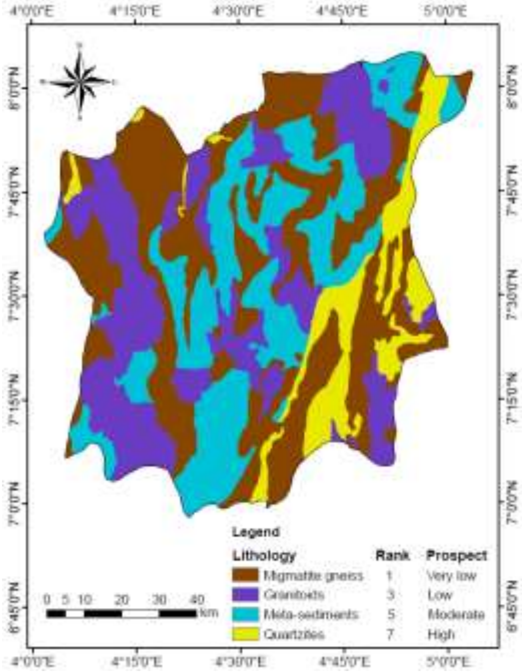

Fig. 4 Potentiality map of lithology

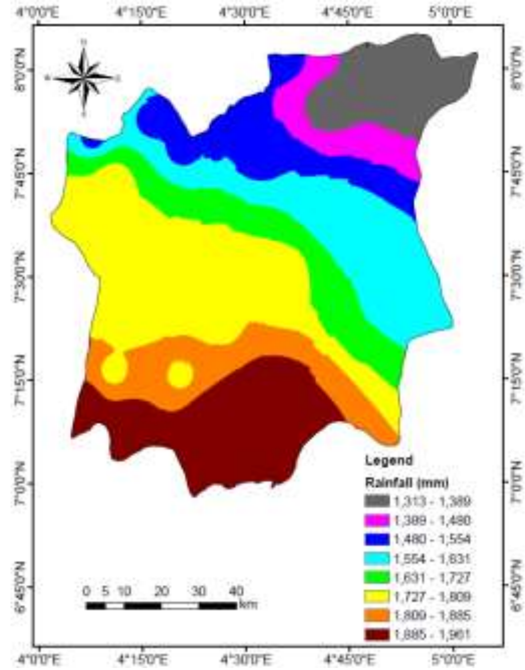

Fig. 5 Spatial distribution of mean annual rainfall

The reclassified rainfall map indicated four groundwater potentiality zones, viz., very low (< 1,450 mm/year), low (1,450 – 1,650 mm/year), high (1,650 – 1,850 mm/year) and very high (>1,850) (Figure 6). These corresponded to 1106.58 km^2 (12.04%), 2720.38 km^2 (29.60%), 3666.41 km^2 (39.90%) and 1695.94 km^2 (18.46%) of the study area respectively (Table 4). Assuming minimum spatial variation in rainfall duration and intensity, this trend in rainfall values suggest that potential for groundwater increased from Northern part to southern part of the area.

3.1.3 Soil media

Soil media in the study area comprises tropical weathering products derived from crystalline basement rocks. The significance of soil media in groundwater prospecting in the hard rock terrain of southwestern Nigeria cannot be overstated because shallow dug wells which serve as source of water for domestic uses in the area tap water from the soil media overlying the basement complex rocks. Crystalline and coarse-grain rocks such as gneiss and migmatite are expected to be sandy and form aquifer when they are weathered. However, argillaceous meta-sediments turn clayey and impermeable when weathered, to form aquiclude. Soil media in the study area comprises sandy clay-loam, clay-sand and silt clay (Figure 7). Their groundwater potentiality was categorized into three, namely, very high, high and low, covering 7442.87 km^2 (6.52%), 723.01 km^2 (46.06%) and 1024.14 km^2 (47.42%) of the landmass respectively (Table 4).

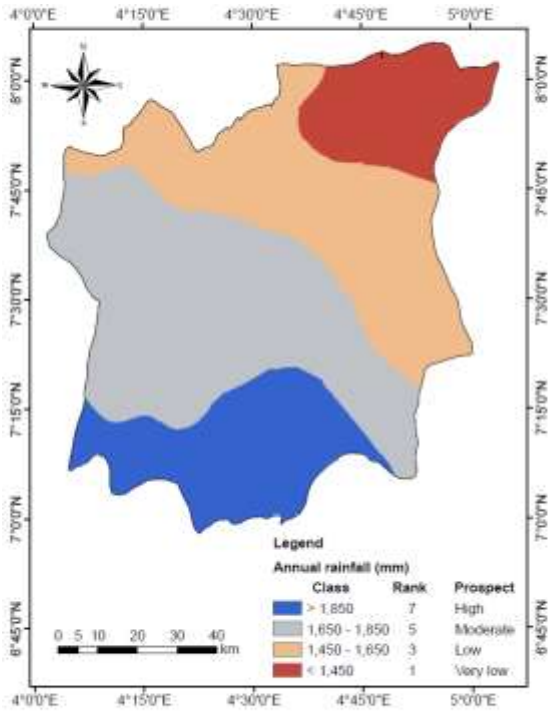

Fig. 6 Potentiality map of rainfall

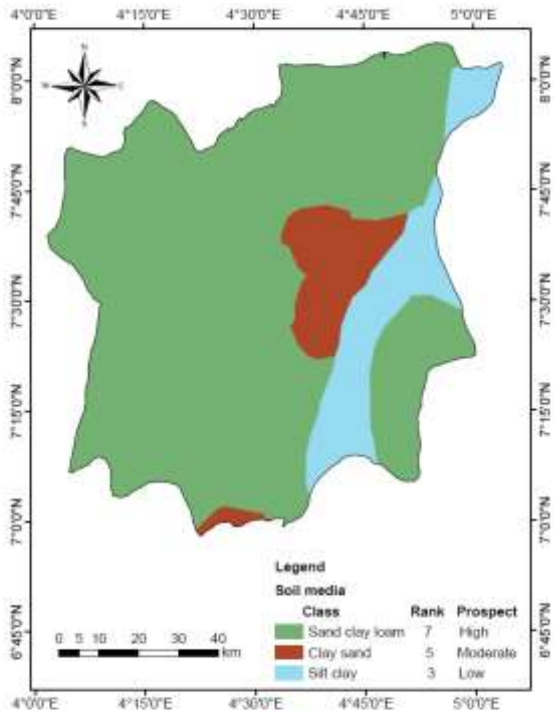

Fig. 7 Potentiality map of soil

3.1.4 Slope angle

Slope angle is a crucial decision criterion which affects drainage density, rate of infiltration and surface runoff and baseflow (Aluko and Igwe, 2019). The rate of runoff increases with increasing slope angle while the rate of infiltration reduces at the same time. In the current study, the slope map indicates widely varied land surface relief with slope angle ranging between 0 and 62.31 degrees (Figure 8). The land slopes were categorized to four classes according to groundwater potentiality, namely, very low (>30^o), low (15^o – 30^o), moderate (5^o – 15^o), and high (<5^o) (Figures 9). The high and moderately high potential zones covered 6885.74 km^2 (60.33%), and 2053.98 km^2 (18%) respectively (Table 4).

Table 4 Evaluation factors and their ratings

Criteria	Criteria Normalized Weight (W_i)	Class	Assigned weight	Feature Normalized weight (w_j)	Groundwater potentiality	Area (km^2)	Area (%)
Lithology	0.3737	Quartzites	7	0.438	High	936.76	10.21
		Meta-sediments	5	0.313	Moderate	2363.52	25.75
		Granitoids	3	0.188	Low	2339.97	25.49
		Migmatite Gneiss	1	0.063	Very low	3538.04	38.55
Rainfall (mm)	0.1101	> 1,850	7	0.438	High	1695.94	18.46
		1,650 – 1,850	5	0.313	Moderate	3666.41	39.90
		1,450 – 1,650	3	0.188	Low	2720.38	29.60
		< 1,450	1	0.063	Very low	1106.58	12.04
Soil media	0.0962	Sand clay loam	7	0.467	High	7442.87	6.52

		Clay sand Silt clay	5 3	0.333 0.200	Moderate Low	723.01 1024.14	46.06 47.42
Slope angle (°)	0.0387	< 5 5 – 15 15 – 30 > 30	7 5 3 1	0.438 0.313 0.188 0.063	High Moderate Low Very low	6885.74 2053.98 234.36 12.95	60.33 18.00 20.53 1.14
Lineament density (km/km²)	0.0900	> 0.15 0.10 – 0.15 0.05 – 0.10 < 0.05	7 5 3 1	0.438 0.313 0.188 0.063	High Moderate Low Very low	2310.44 1750.66 1401.12 3727.08	25.14 19.05 15.25 40.56
Land use/cover	0.0637	Wetlands/water Vegetation Built-up areas Rock/bare surface	7 5 3 1	0.438 0.313 0.188 0.063	High Moderate Low Very low	35.10 6215.59 515.96 2422.66	2.48 43.93 36.47 17.12
Altitude (m)	0.0978	68 - 222 222 – 313 313 – 436 436 - 768	1 3 5 7	0.063 0.188 0.313 0.438	Very low Low Moderate High	2453.38 3347.67 2663.87 721.94	15.64 21.34 16.98 46.03
Topographic wetness Index	0.0189	2.75 – 7.31 7.31 – 9.95 9.95 – 13.89 13.89 – 25.12	7 5 3 1	0.438 0.313 0.188 0.063	High Moderate Low Very low	5177.23 2586.91 1149.23 273.66	44.44 22.21 9.86 23.49
Drainage density (km/km²)	0.0636	0 – 0.15 0.15 – 0.30 0.30 – 0.45 0.45 – 1.59	7 5 3 1	0.438 0.313 0.188 0.063	High Moderate Low Very low	2283.28 1975.92 1354.45 3575.66	24.85 21.50 14.74 38.91
Proximity to river/stream (km)	0.0472	0 – 100 100 – 200 200 – 300 300 – 7,206	7 5 3 1	0.438 0.313 0.188 0.063	High Moderate Low Very low	469.03 423.07 455.51 7841.70	22.00 19.85 21.37 36.78

3.1.5 Lineament density

Occurrence of groundwater in the hard rock terrain depends largely on distribution of structural features that create secondary porosity in the rocks. Appropriate siting of high-yielding water boreholes in such terrain depends on proper delineation of the locations of these buried linear structures (fractures and joints) serving as reservoir rocks, and groundwater prospect zones. Appreciable length, depth and frequency of lineaments enhance potential of impermeable hard rocks for water storage. Besides, points of intersection of two or more fractures form a conduit for groundwater. Higher lineament density is associated with greater groundwater potential of the zone. Hence, these lineaments are often the targets when prospecting for water in such hard rock terrains. Figure 10 shows the lineament map for the study area. Greater lineament density translates to higher potential for groundwater storage. The lineament density for the study area was classified into four groundwater potential zones, namely, high (> 0.15 km/km^2), moderate (0.10 - 0.15 km/km^2), low (0.05 – 0.10 km/km^2) and very low (< 0.05 km/km^2) (Figure 11). High and moderately high potential zones covered 2310.44 km^2 (25.14%), and 1750.66 km^2 (19.05%) respectively (Table 4).

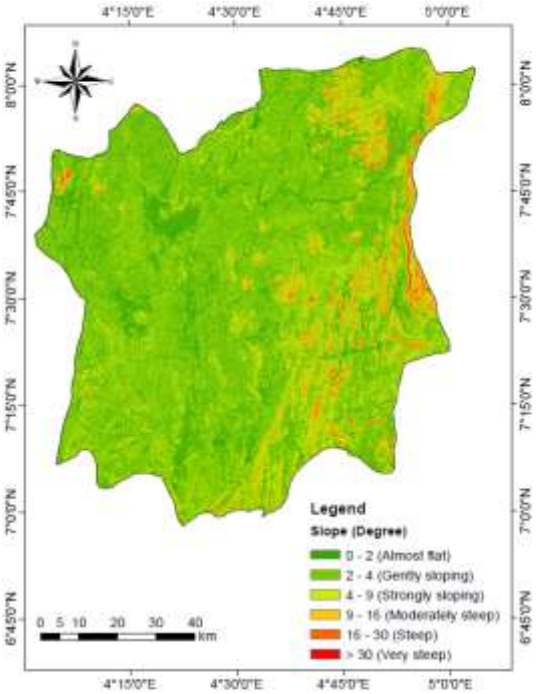

Fig. 8 Slope map

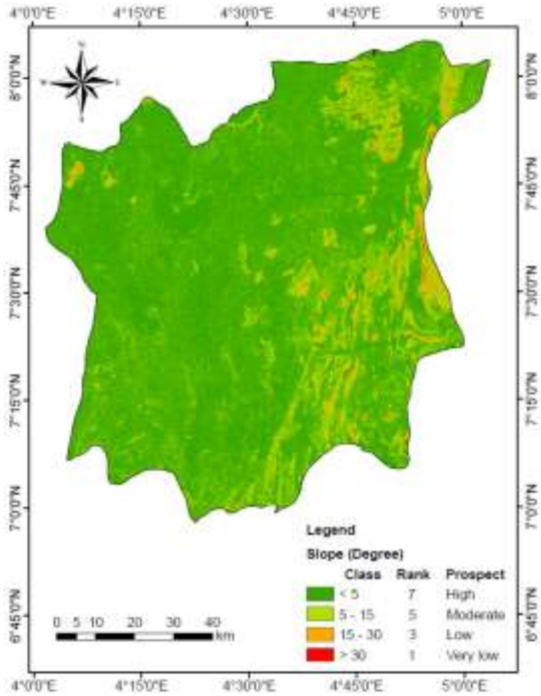

Fig. 9 Potentiality map of slope

3.1.6 Land use

Land use/land cover (LULC) is an important factor that influences groundwater discharge and recharge rates. LULC enhances or prevents infiltration, evaporation/evapotranspiration and surface runoff. The various LULC in the study area were categorized into four classes, namely, wetlands/water bodies, built-up areas, rock outcrops/bare surfaces, and vegetation. The classes were ranked on a 4-point scale of groundwater potentiality, viz., very low (1), low (3), moderate (5) and high (7) (Figure 12). Rock outcrops impede rainwater infiltration, thereby reducing possibility of groundwater recharge. Wetlands and vegetation classes were assigned high weights because of wide surface area favourable for high infiltration. Hence, such areas indicated high and moderately high groundwater potential zones with area coverage of 35.10 km^2 (2.48%) and 6215.59 km^2 (43.93%) respectively (Table 4).

3.1.7 Altitude

Altitude is a key factor controlling groundwater recharge in an area (Pourtaghi & Pourghasemi 2014). The range of altitude in the study area is between 68 m and 768 m above the mean seal level. The altitude was classified into four classes, viz., 68-222 m, 222 – 313 m, 313 – 436 m, and 436 – 768 m, representing as very low, low, moderate, and high groundwater potentiality respectively (Figure 13). These classes covered 2453.38 km^2 (15.64%), 3347.67 km^2 (21.34%), 2663.87 km^2 (16.98%) and 721.94 km^2 (46.03%) of the study area respectively (Table 4).

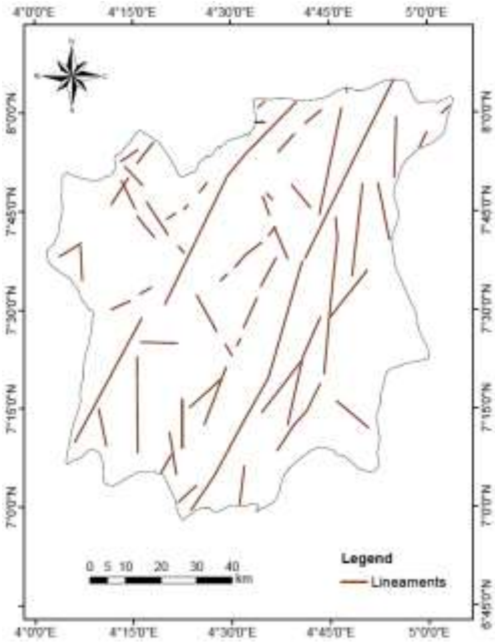

Fig. 10 Lineament map (NGSA, 2006b)

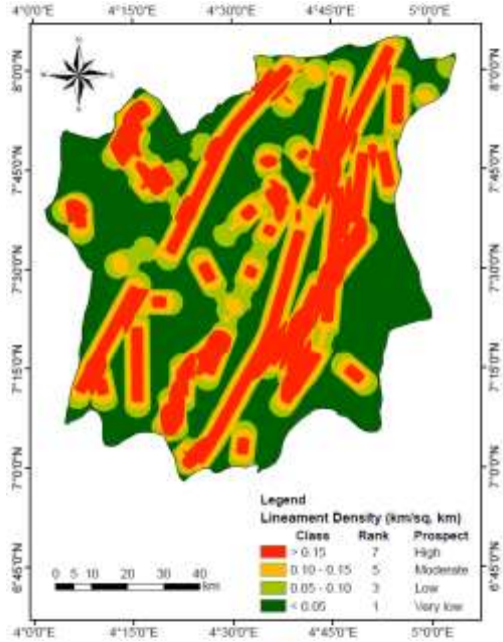

Fig. 11 Potentiality map of lineament density

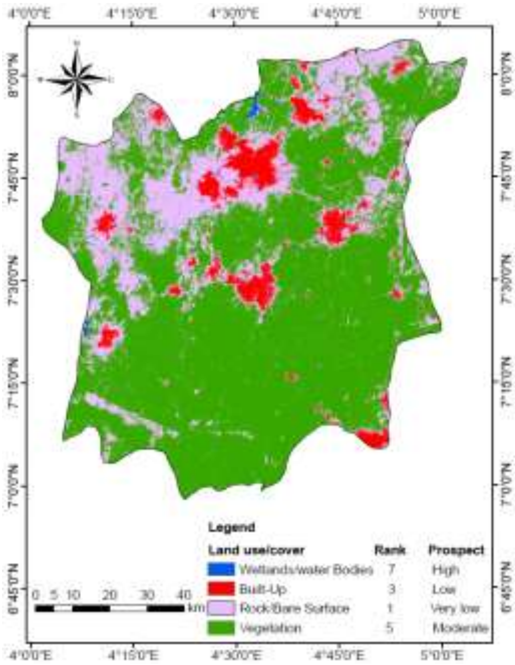

Fig. 12 Potentiality map of land use/cover

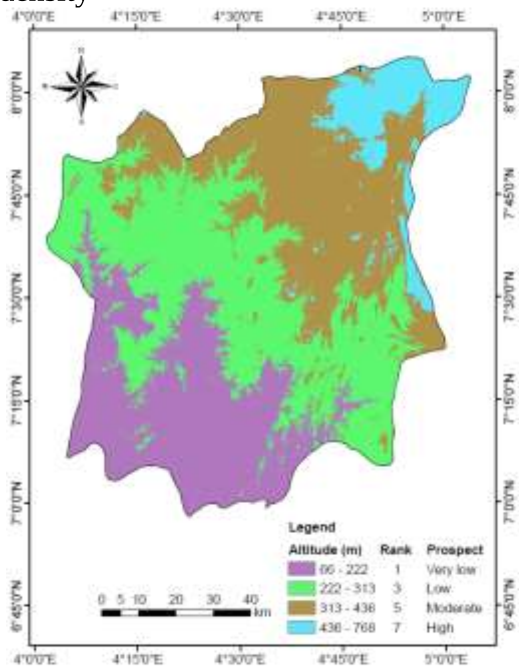

Fig. 13 Potentiality map of altitude

3.1.8 Topographic wetness index

Topographic wetness index (TWI) is the likelihood that soils in an area will be saturated based on the slope characteristics of the surrounding area, and the porosity of the ground surface (Razandi et al, 2015). The greater the index value, the less the potentiality for groundwater storage. The TWI values for the study area varied from 2.75 to 25.12 and were classified into, high (2.75-7.31), moderate (7.31-9.95), low (9.95-13.89), and very low (13.89-25.12) groundwater potential zones according to Jenks' natural breaks (Figure 14). The high and moderately high potential zones covered land area of 5177.23 km^2 (44.44%) and 2586.91 km^2 (22.21%) respectively (Table 4).

3.1.9 Drainage density

Drainage density is considered one of the important factors indicating possible groundwater storage in an area. Drainage density enhances groundwater discharge and reduces recharge potentials. Hence, high drainage density lowers the chances of infiltration and decreases groundwater recharge. For groundwater prospect in the study area, the drainage density derived from the drainage map (Figure 15), was grouped into four, namely, 0-0.15 km/km^2 (high), 0.15-0.30 km/km^2 (moderate), 0.30-0.45 km/km^2 (low), and 0.45-1.59 km/km^2 (very low) (Figure 16). About 2283 km^2 (24.85%) and 1976 km^2 (21.50%) of land areas indicated high and moderately high groundwater potentiality respectively, totalling 4259 km^2 (46%) of the study area (Table 4).

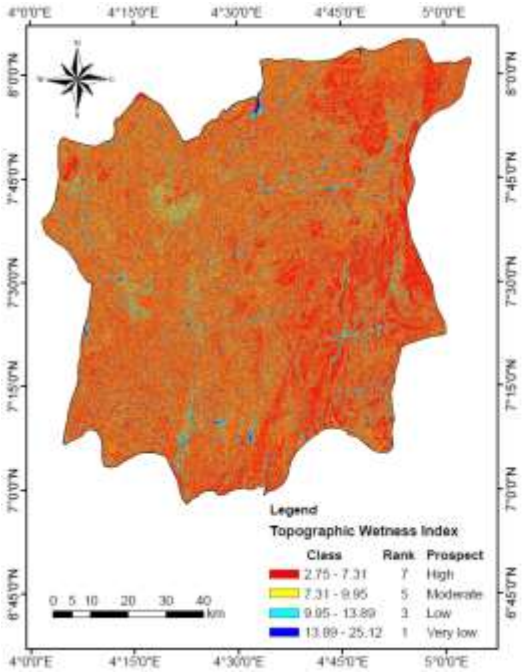

Fig. 14 Potentiality map of TWI

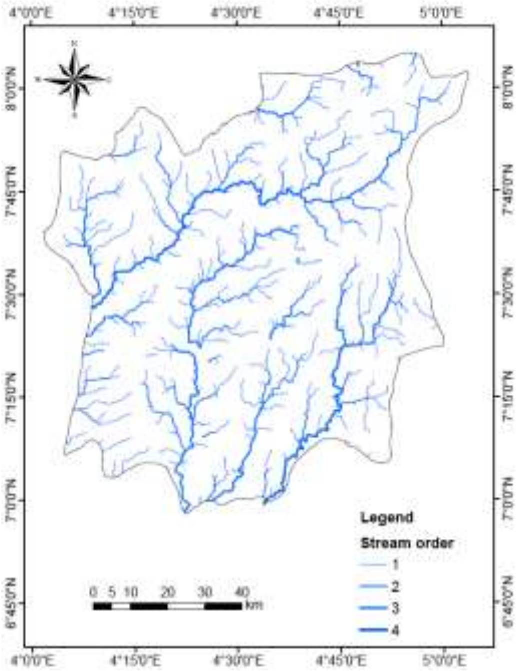

Fig. 15 Stream order map

3.1.10 Proximity to Rivers and streams

Proximity to rivers and streams is a conditioning factor to consider on surface-groundwater dynamics, and potential for groundwater recharge. Effluent flow condition enhances groundwater recharge while influent condition enhances groundwater discharge. The flow condition in the study area was considered effluent, and buffer zones closest to rivers/streams were assigned the highest weight of 4, and buffer zones farthest got the lowest weight of 1, indicating highest and lowest potentiality for groundwater recharge respectively. Four classes of buffer zones were identified, namely, 0-100 km (high), 100-200 km (moderate), 200-300 (low), and > 300 (very low) (Figure 17). The high potentiality zone covered 469.03 km^2 (22.00%) while the moderately high potentiality zone is 423.07 km^2 (19.85%) (Table 4).

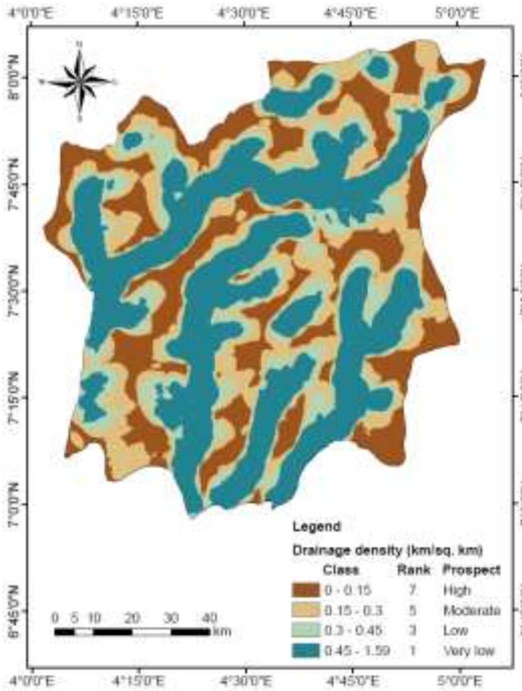

Fig. 16 Potentiality map of drainage density

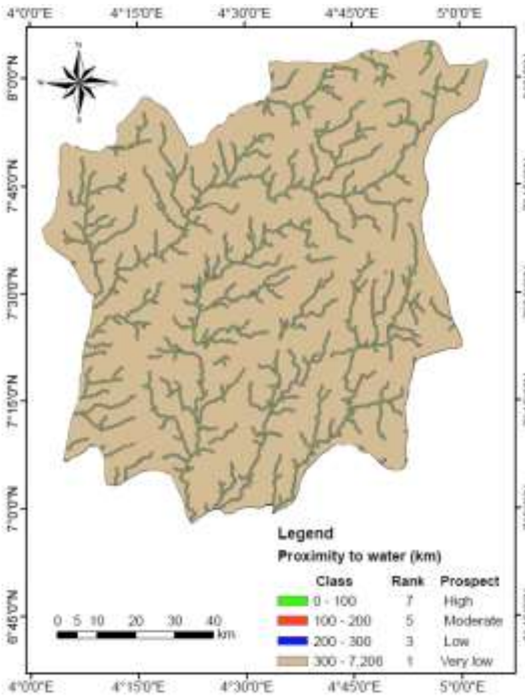

Fig. 17 Potentiality map of drainage proximity

3.2 Application of Analytical Hierarchical Process (AHP) model

Table 5 shows the result of pairwise comparison matrix for the ten groundwater conditioning factors considered most appropriate for groundwater potential mapping in the study area. The result of AHP indicated that the lithology has the highest normalized weight while topographic wetness index has the least weight. The order of influence of the conditioning factors from the highest to the least is as follows: lithology (37.4%), rainfall (11%), altitude (9.8%), soil (9.6%), lineament density (9.0%), land use (6.4%), drainage density (6.4%), drainage proximity (4.7%), slope (3.9%), and topographic wetness index (1.9%). The value of Principal Eigenvalue (λ_{max}) and Consistency Index (CI) obtained for the pair-wise comparison matrix are 10.1426 and 0.0158 respectively. The value of Consistency Ratio (CR) is 0.011, an indication that the comparison matrix was reasonably consistent, having recorded a value that falls within the acceptable range (CR $\leq$ 0.1).

Figure 18 shows the final groundwater potential map for AHP model with indication of high potentiality towards areas underlain by quartzite and meta-sediments, and where lineament density was high in the study area. Very low groundwater potential zones coincide with areas underlain by migmatite-gneiss and granitoids, and characterized by low lineament density. Four groundwater potential zones were delineated, namely, very low, low, moderate and high, and the respective zones covered 47.29 km^2 (0.52%), 6238.53 km^2 (68.09%), 2864.25 km^2 (31.26%), and 12.22 km^2 (0.13%) (Table 7).

Table 5 The pairwise comparison matrix for evaluation criteria and relative weight for AHP

Factors	LG	RN	SM	SA	LD	LU	AT	TW	DD	DP	Normalized Weight
LG	1										0.3737
RN	0.33	1									0.1101
SM	0.20	1.00	1								0.0962
SA	0.11	0.33	0.40	1							0.0387
LD	0.25	0.75	1.00	2.25	1						0.0900
LU	0.17	0.50	0.60	1.50	0.67	1					0.0637
AT	0.25	1.00	1.00	2.50	1.00	2.00	1				0.0978
TW	0.05	0.20	0.20	0.50	0.20	0.33	0.20	1			0.0189
DD	0.17	0.50	0.60	1.50	0.67	1.00	0.67	3.33	1		0.0636
DP	0.14	0.50	0.50	1.50	0.67	0.33	0.57	3.33	0.50	1	0.0472

Principal Eigenvalue (λ_{max}) = 10.1426, Random Index (RI) = 1.49, Consistency Index (CI) = 0.0158, Consistency Ratio (CR) = 0.011. Lithology (LG), Rainfall (RN), Soil media (SM), Slope angle (SA), Lineament density (LD), Land use (LU), Altitude (AT), Topographic wetness (TW), Drainage density (DD), Drainage proximity (DP)

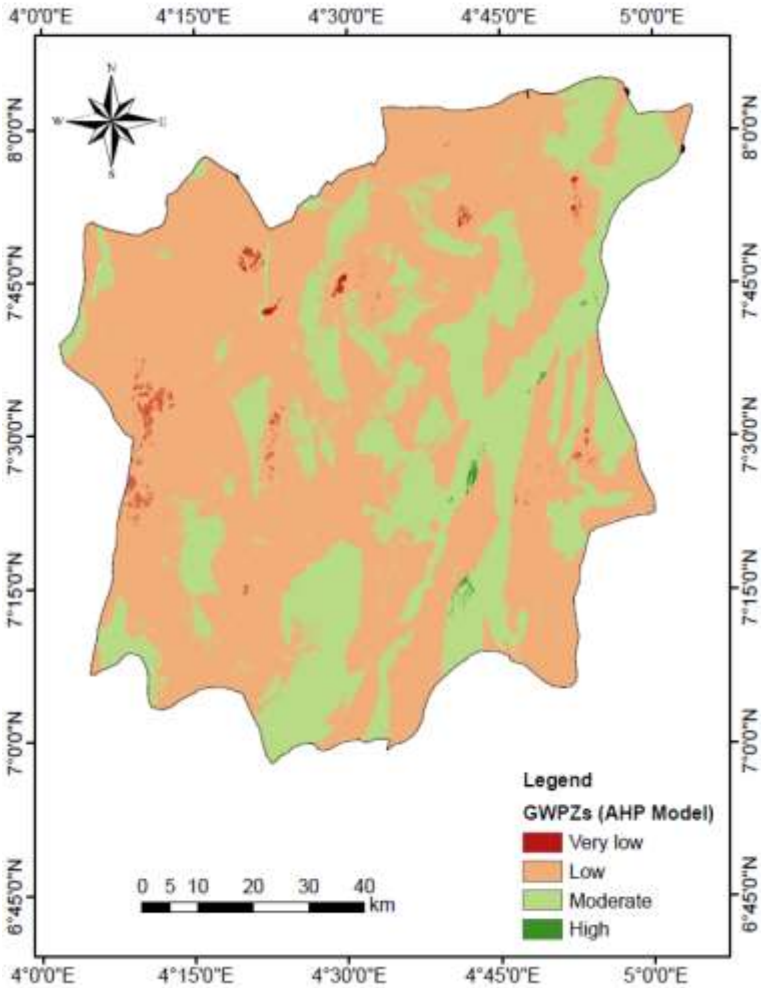

Fig. 18 Groundwater potential map for AHP model

3.3 Application of Frequency Ratio (FR) model

Table 6 shows the results of the spatial relationship between evaluation criteria and groundwater well locations, using Frequency Ratio (FR) model.

Table 6 Spatial relationship between evaluation criteria and well locations using FR model

Thematic layers	Classes	No. of pixels in classes	Percentage of pixels in classes *(a)*	No. of well pixels	Percentage of well pixels *(b)*	FR = $\frac{b}{a}$
Lithology	Quartzites	104084	10.21	9	15.79	1.546
	Meta-sediments	262613	25.75	16	28.07	1.090
	Granitoids	259996	25.49	8	14.04	0.551
	Migmatite Gneiss	393115	38.55	24	42.11	1.092
Rainfall (mm)	> 1,850	188437	18.46	0	0..00	0
	1,650 – 1,850	407379	39.90	11	19.30	0.484
	1,450 – 1,650	302264	29.60	31	54.39	1.837
	< 1,450	122952	12.04	15	26.32	2.186
Soil media	Sand clay loam	113793	6.52	11	19.30	2.960
	Clay sand	803345	46.06	9	15.79	0.343
	Silt clay	826985	47.42	37	64.91	1.369
Slope angle (°)	< 5	765081	60.33	48	84.21	1.396
	5 – 15	228220	18.00	8	14.04	0.780
	15 – 30	260401	20.53	1	1.754	0.085
	> 30	14394	1.14	0	0.00	0
Lineament density (km/km^2)	> 0.15	256715	25.14	14	24.56	0.977
	0.10 – 0.15	194518	19.05	12	21.05	1.105
	0.05 – 0.10	155680	15.25	10	17.54	1.150
	< 0.05	414120	40.56	21	36.84	0.908
Land use/cover	Wetlands/water	38996	2.48	4	7.018	2.830
	Vegetation	690621	43.93	25	43.86	0.998
	Built-up areas	573284	36.47	13	22.81	0.625
	Rock/bare surface	269184	17.12	15	26.32	1.537
Altitude (m)	68 - 222	272598	15.64	2	3.51	0.224
	222 – 313	371963	21.34	14	24.56	1.151
	313 – 436	295985	16.98	35	61.40	3.616
	436 - 768	802160	46.03	6	10.53	0.229
Topographic wetness Index	2.75 – 7.31	575247	44.44	24	42.11	0.947
	7.31 – 9.95	287434	22.21	21	36.84	1.659
	9.95 – 13.89	127692	9.86	10	17.54	1.779
	13.89 – 25.12	304069	23.49	2	3.51	0.149
Drainage density (km/km^2)	0 – 0.15	253697	24.85	12	21.05	0.847
	0.15 – 0.30	219546	21.50	16	28.07	1.306
	0.30 – 0.45	150494	14.74	5	8.77	0.595
	0.45 – 1.59	397295	38.91	24	42.11	1.082
Proximity to river/stream (km)	0 – 100	521142	22.00	2	3.51	0.159
	100 – 200	470076	19.85	1	1.75	0.088
	200 – 300	506124	21.37	5	8.77	0.410

	300 – 7,206	871300	36.78	49	85.96	2.337

According to Lee and Pradhan (2006), the correlation is low if FR value is less than 1, and it suggests low groundwater potential. The correlation is high when FR value is greater than 1 and it indicates high groundwater potential. For lithology, the quartzites class recorded the highest FR value of 1.546 while the granitoids class has the lowest value of 0.551.Hence the quartzite has the highest probability for groundwater occurrence, whereas, granitoids possess the least potential. For rainfall, the < 1,450 class has the highest FR value of 2.186, followed by 1,450 - 1,650 class with the value of 1.837. Both 1,650 – 1,850 and > 1,850 classes have FR values less than 1, implying low groundwater potential. For soil, sand-clay-loam has FR value of 2.960 while clay-sand and silt-clay recorded FR values of 0.343 and 1.369 respectively. This suggests that the sand-clay-loam has the highest probability for groundwater potential.

In the case of slope angle, < 5 class with the highest value of FR (1.396), has the highest correlation, and groundwater potential. The lineament density classes 0.10 - 0.15 and 0.05 – 0.10 indicate high correlation with FR values of 1.105 and 1.150, thereby suggesting high groundwater potential. The < 0.05 and > 0.15 classes have values of FR (0.908 and 0.977 respectively) which are less than 1, and are therefore considered as having low groundwater potential. In the case of altitude, most groundwater occurred in the range of altitude between 313 – 436 m and 222 – 312 m. For TWI, 7.31-9.95 and 9.95-13.89 classes had FR > 1, indicating high groundwater potential, while 2.75-7.31 and 13.89-25.12 classed gave FR < 1, indicating low groundwater potential. In the case of drainage density, 0.15-0.30 and 0.45-1.59 classes had FR >1 and are high in groundwater potential. However, the 0-0.15 and 0.30-0.45 classes had FR < 1 and are low in groundwater potential. For proximity to streams, only the 300-7,206 class had FR value greater than 1. Hence, only this class had high groundwater potential while the remaining classes had low potentials for groundwater.

Figure 19 shows the final groundwater potential map for FR model. Four groundwater potential zones were delineated, namely, very low, low, moderate and high, and they covered 14.26 km^2 (0.16%), 5004.85 km^2 (54.62%), 4092.74 km^2 (44.67%), and 50.45 km^2 (0.55%) respectively (Table 7).

Table 7 Summary of groundwater potential zones using AHP and FR models

Groundwater Potential	AHP		FR	
	Area (km^2)	Percentage	Area (km^2)	Percentage
Very low	47.29	0.52	14.26	0.16
Low	6238.53	68.09	5004.85	54.62
Moderate	2864.25	31.26	4092.74	44.67
High	12.22	0.13	50.45	0.55

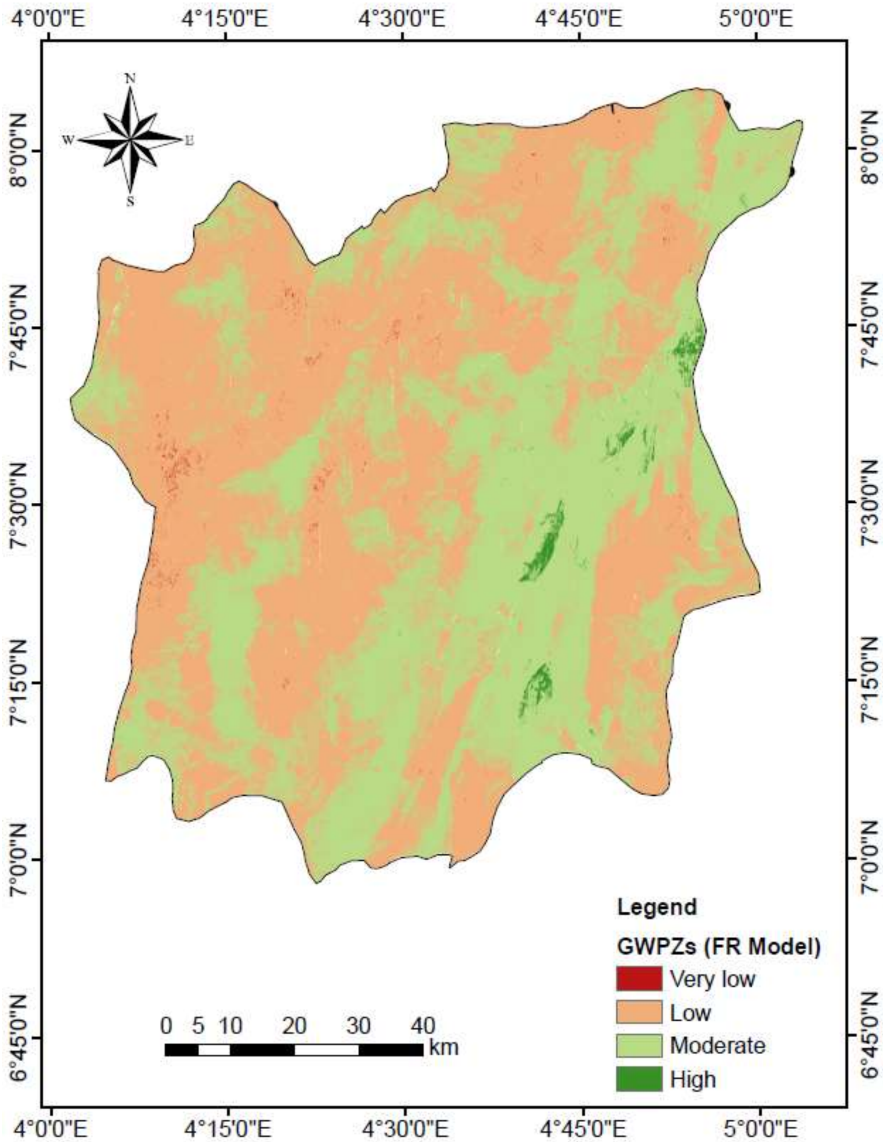

Fig. 19 Groundwater potential map for FR model

3.4 Validation of groundwater potential maps

As a way of ascertaining prediction accuracy of the AHP and FR models adopted in the study, model validation became necessary. The receiver operating characteristics (ROC) curve which was implemented depicts the trade-off between the false positive rate, and the true positive rate, plotted on the X-axis and Y-axis respectively (Cervi et al., 2010). The validation results of the groundwater potential maps generated in the current study indicated that the AUC for the AHP model was 0.731 while that of the FR model was 0.717 (Figures 20 and 21). Hence, their prediction accuracies are 73.1% and 71.7% respectively. According to Yesilacar (2005) and Pourghasemi et al. (2012), both models showed reasonably good prediction accuracy of groundwater productivity in the study area.

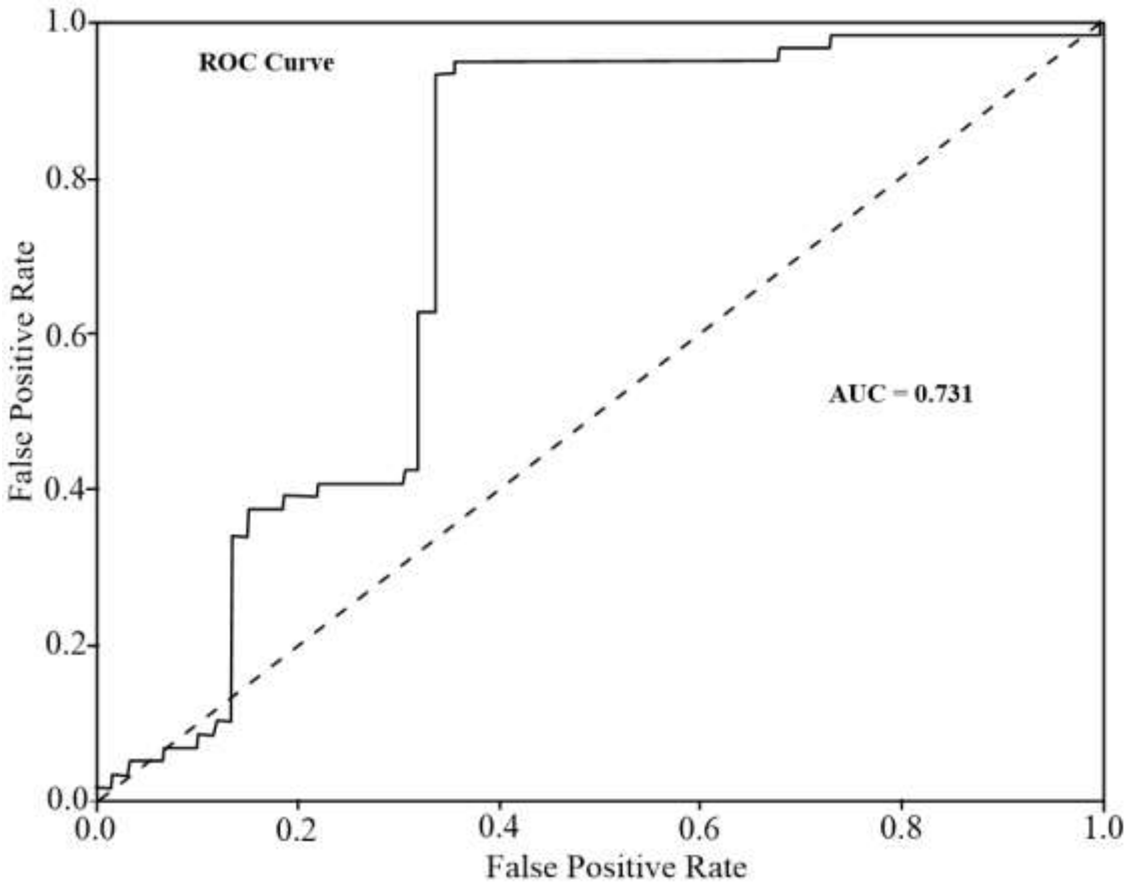

Fig. 20 Receiver Operating Characteristics (ROC) curve for GWPZ map from AHP model

4. CONCLUSION

The knowledge-based analytic hierarchy process (AHP) and the data-driven frequency ratio (FR) have been used for GIS-based integration of most applicable groundwater conditioning factors to generate groundwater potential maps for the hard rock terrain of Osun State, Nigeria. The results of AHP method indicated that the order of influence of the conditioning factors on groundwater potential is, lithology > rainfall > altitude > soil > lineament density > land use > drainage density > drainage proximity > slope angle > topographic wetness index. The validation results from ROC analysis revealed that both the AHP and FR models have good prediction accuracies of 73.1% and 71.7% respectively. Hence, the groundwater potential maps produced could serve as tools in decision making on land use planning and groundwater resources development in the area. The model results agree well with the findings of earlier workers in similar terrain (Fashae et al., 2014; Aluko and Igwe, 2017).

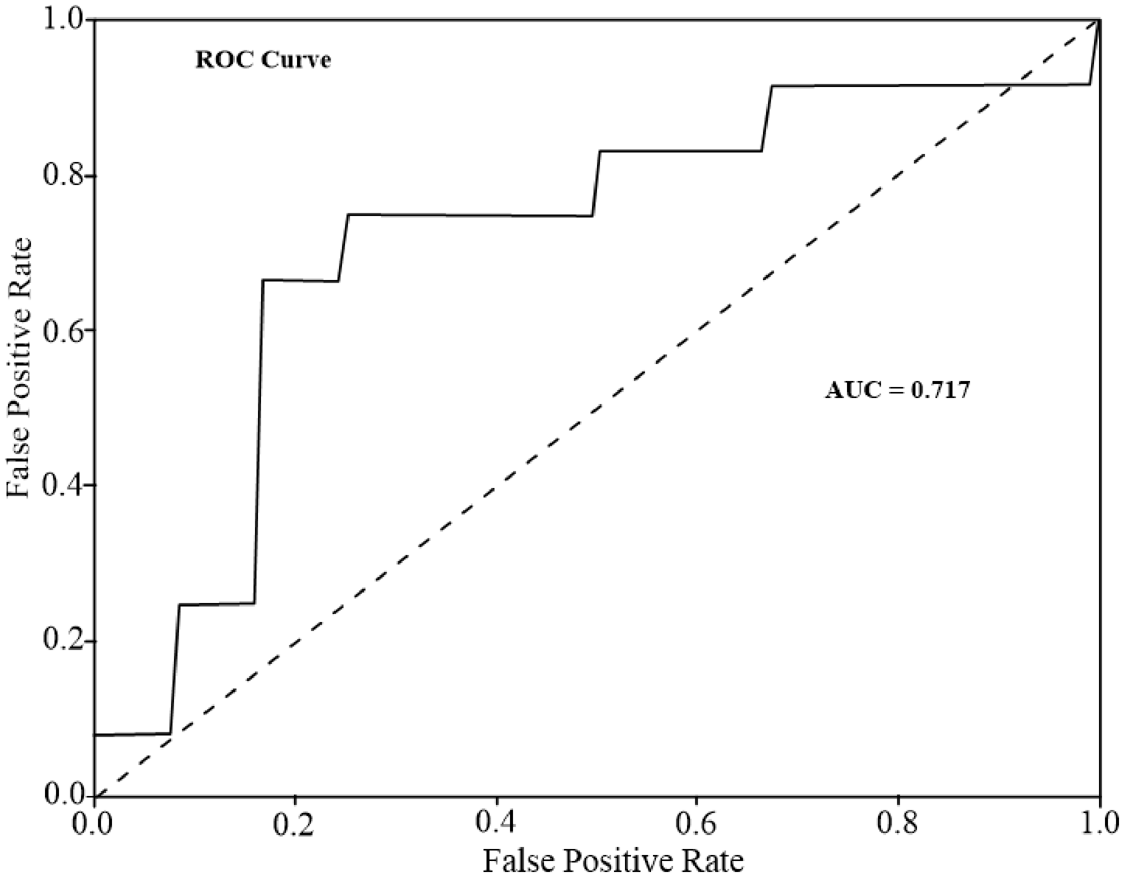

Fig. 21 Receiver Operating Characteristics (ROC) curve for GWPZ map from FR model

REFERENCES

Abdulazeez, A., & Naisa, A. G. (2018). An Appraisal of Factors Affecting Groundwater Formation and Recharge in Parts of Northern Kano State, Nigeria.

Abijith, D., Saravanan, S., Singh, L., Jennifer, J. J., Saranya, T., & Parthasarathy, K. S. S. (2020). GIS-based multicriteria analysis for identification of potential groundwater recharge zones – a case study from Ponnaniyaru watershed, Tamil Nadu, India. *HydroResearch,* 3, 1 – 14.

Abrams, W., Ghoneim, E., Shew, R., LaMaskin, T., Al-Bloushi, K., Hussein, S., AbuBakr, M., Al-Mulla, E., Al-Awar, M., & El-Baz, F. (2018). Delineation of groundwater potential (GWP) in the northern United Arab Emirates and Oman using geospatial technologies in conjunction with simple additive weight (SAW), analytical hierarchy process (AHP), and probabilistic frequency ratio (PFR) techniques. *Journal of Arid Environment.* 157, 77–96. https://doi.org/10.1016/j.jaridenv.2018.05.005

Adekoya, J. A., Kehinde-Philips, O. O., & Odukoya, A. M. (2003). Geological distribution of mineral resources in southwestern Nigeria. In: A. A. Elueze (ed). Prospects for investment in mineral resources of southwestern Nigeria, pp. 1 – 13.

Adiat, K. A. N., Nawawi, M. N. N., & Abdullah, K. (2013) Application of multicriteria decision analysis to geoelectric and geologic parameters for spatial prediction of groundwater resources potential and aquifer evaluation. *Pure Applied Geophysics* 170:453–471

Afshar, A., Abedi, M., Norouzi, G.-H., & Riahi, M.-A. (2015). Geophysical investigation of underground water content zones using electrical resistivity tomography and ground penetrating radar: A case study in Hesarak-Karaj, Iran. *Engineering Geology*, 196, 183–193. doi:10.1016/J.ENGGEO.2015.07.022.

Akinluyi, F. O. (2013). Integration of Remotely Sensed and Geophysical Data in Groundwater Potential Evaluation of the Basement Complex Terrain of Ondo State, Southwestern Nigeria. An Unpublished Ph.D Thesis, Dept. of Geology, OAU, Ile-Ife, Nigeria.

Akinwumiju, A. S., & Olorunfemi, M. O. (2016). Shallow aquifer characteristics, borehole yield and Groundwater resource sustainability assessment in the Osun Drainage basin, southwestern Nigeria. *Ife Journal of Science.* 18(2), 305-314.

Al-Abadi, A. M. (2015). Groundwater potential mapping at north-eastern Wasit and Missan governorates, Iraq using a data-driven weights of evidence technique in framework of GIS. *Environmental Earth Science.* https://doi.org/10.1007/s12665-015-4097-0

Al-Djazouli, M. O., Elmorabiti, K., Rahimi, A., Amellah, O., & Fadil, O. A. M. (2020). Delineating of groundwater potential zones based on remote sensing, GIS and analytical hierarchical process: a case of Waddai, eastern Chad. *GeoJournal.* 5, 1-14. https://doi.org/10.1007/s10708-020-10160-0

Al-Djazouli, M. O., Elmorabiti, K., Zoheir, B., et al. (2019). Use of Landsat-8 OLI data for delineating fracture systems in subsoil regions: Implications for groundwater prospection in the Waddai area, eastern Chad. *Arabian Journal of Geosciences,* 12(7), 241. https://doi:10.1007/s12517-019-4354-8

Aluko, O. E., & Igwe, O. (2017). An integrated geomatics approach to groundwater potential delineation in the Akoko-Edo Area, Nigeria. *Environmental Earth Science* 76:240. https://doi.10.1007/s12665-017-6557-1

Andualem, T. G.., and Demeke, G. G. (2019). Groundwater potential assessment using GIS and remote sensing: A case study of Guna tana landscape, upper blue Nile Basin, Ethiopia. *Journal of Hydrology: Regional Studies.* 24, https://doi.org/10.1016/j.ejrh.2019.100610

Arshad, A., Zhang, Z., Zhang, W., & Dilawar, A. (2020). Mapping favourable groundwater potential recharge zones using a GIS-based analytical hierarchical process and probability frequency ratio model: A case study from an agro-urban region of Pakistan. *Geoscience Frontiers.* https://doi.org/10.1016/j.gsf.2019.12.013

Arulbalaji, P., Padmalal, D., & Sreelash, K. (2019). GIS and AHP techniques-based delineation of groundwater potential zones: a case study from southern Western Ghats, India. *Scientific Reports.* 9 (1), 1–17.

Cervi, F., Berti, M., Borgatti, L., Ronchetti, F., Manenti, F., & Corsini, A. (2010). Comparing predictive capability of statistical and deterministic methods for landslide susceptibility mapping: A case study in the northern Apennines (Reggio Emilia Province, Italy). *Landslide*, 7(4), 433–444.

Chowdhury, A., Jha, M. K., Chowdary, V. M., & Mal, B. C. (2009). Integrated remote sensing and GIS-based approach for assessing groundwater potential in West Medinipur district, West Bengal, India. *International Journal of Remote Sensing*, 30(1), 231–250. https://doi:10.1080/01431160802270131

Davoodi Moghaddam D, Rezaei M, Pourghasemi HR, Pourtaghie ZS, Pradhan B (2013) Groundwater spring potential mapping using bivariate statistical model and GIS in the taleghan watershed Iran. *Arab Journal of Geoscience* https://doi:10.1007/s12517-013-1161-5

Day-Lewis, F. D., Slater, L. D., Robinson, J., et al. (2017). An overview of geophysical technologies appropriate for characterization and monitoring at fractured-rock sites. *Journal of Environmental Management*, 204, 709–720. doi:10.1016/J.JENVMAN.2017.04.033.

Dı´az-Alcaide, S., Martı´nez-Santos, P. (2019). Review: Advances in groundwater potential mapping. *Hydrogeology Journal*, 27(7), 2307–2324.

Earman, S. & Dettinger, M. (2011). Potential impacts of climate change on groundwater resources – a global review. *Journal of water and climate change,* 2(4), 213-229. https://doi.org/10.2166/wcc.2011.034

Elueze, A. A. 2002. Compositional character: Veritable tool in the appraisal of Geomaterials. An inaugural lecture, University of Ibadan. 43pp

Fashae, O. A., Tijani, M. N., Talabi, A. O., & Adedeji, O. I. (2014). Delineation of groundwater potential zones in the crystalline basement terrain of SW-Nigeria: an integrated GIS and remote sensing approach. *Applied Water Science.* 4, 19–38. https://doi.org/10.1007/s13201-013-0127-9

Foster, S.S.D., Lawrence, A.R and Morris, B.M. (1998). Groundwater in urban development. World Bank Technical Paper, no 390, Washington DC, USA.

Hamdani, N. & Baali, A (2020). Characterization of groundwater potential zones using analytic hierarchy process and integrated geomatic techniques in Central Middle Atlas (Morocco). *Applied Geomatics*. https://doi.org/10.1007/s12518-020-00300-z

Hughes, A., Mansour, M., Ward, R., Kieboom, N., Allen, S., Seccombe, M., & Charlton, C. P. (2021). The impact of climate change on groundwater recharge: National-scale assessment for the British mainland. *Journal of Hydrology.* 598, 1-14, https://doi.org/10.1016/j.jhydrol.2021.126336

Jaafari A, Najafi A, Pourghasemi HR, Rezaeian J, Sattarian A (2014) GIS-based frequency ratio and index of entropy models for landslide susceptibility assessment in the Caspian Forest, northern Iran. *International Journal of Environmental Science & Technology.* https://doi:10.1007/s13762-013-0464-0

Kaliraj S, Chandrasekar N, Magesh NS (2014) Identification of potential groundwater recharge zones in Vaigai upper basin, Tamil Nadu, using GIS-based analytical hierarchical process (AHP) technique. *Arabian Journal of Geoscience,* 7(4):1385–1401

Kumar, A., Krishna, A.P., 2018. Assessment of groundwater potential zones in coal mining impacted hard-rock terrain of India by integrating geospatial and analytic hierarchy process (AHP) approach. *Geocarto Int*. 33, 105–129. https://doi:10.1080/10106049.2016.1232314

Lee, S., & Pradhan, B. (2006). Probabilistic landslide hazards and risk mapping on Penang Island, Malaysia. *Journal of Earth System Science* 115(6):661–667.

Malczewski, J., 1999. GIS And Multicriteria Decision Analysis. John Wiley and Sons.

Mogaji, K.A., Lim, H.S., & Abdullah, K. (2015). Modelling of groundwater recharge using a multiple linear regression (MLR) recharge model developed from geophysical parameters: a case of groundwater resources management. *Environmental Earth Science*. 2015 (73), 1217–1230. doi:10.1007/s12665-014-3476-2.

Nampak, H., Pradhan, B., Manap, M.A., 2014. Application of GIS based data driven evidential belief function model to predict groundwater potential zonation. *Journal of Hydrology*. 513, 283–300.

National Population Commission (2009). Federal Republic of Nigeria Official Gazette, Vol. 96, No. 2. Legal Notice on the Publication of 2006 Census Final Results, P.B142. Printed and Published by the Federal Government Printer, Abuja, Nigeria.

Nigerian Geological Survey Agency (2006a). Geological Map of Nigeria, Nigeria Geological Survey Agency, Abuja.

Nigerian Geological Survey Agency (2006b). Lineaments Map of Nigeria, Nigeria Geological Survey Agency, Abuja.

Nwankwoala, H. O. (2014) Problems and options of Integrated water resources management in Nigeria: Administrative constraints and policy strategies. International Letters of Natural Sciences. 9, 12 - 25.

Offodile, M. E. (1992). An approach to groundwater study and development in Nigeria. Mecon services Ltd, Jos Nigeria. 247p.

Oh, H. J., Kim, Y. S., Choi, J. K., Park, E., & Lee, S. (2011) GIS mapping of regional probabilistic groundwater potential in the area of Pohang City, Korea. *Journal of Hydrology.* 399, 158–172.

Olorunfemi, M. O., Ojo, J. S., & Akintunde, O. M. (1999). Hydrogeophysical evaluation of groundwater potentials of Akure metropolis, southwestern Nigeria. *Journal of Mining and Geology.* 35(2), 207-228.

Olorunfemi, M. O., Oni, A. G., Bamidele, O. E., Fadare, T. K., & Aniko, O. O. (2020). Combined geophysical investigations of the characteristics of a regional fault zone for groundwater development in a basement complex terrain of South-west Nigeria. *SN Applied Sciences*, 2:1033. https://doi.org/10.1007/s42452-020-2363-6

Oyedele, A. A. (2019). Use of remote sensing and GIS techniques for groundwater exploration in the basement complex terrain of Ado-Ekiti, SW Nigeria. *Environmental Earth Sciences,* 76:511, 1-20. https://doi:10.1007/s12665-017-6840-1

Pinto, D., Shrestha, S., Babel, M.S., Ninsawat, S., 2017. Delineation of groundwater potential zones in the Comoro watershed, Timor Leste using GIS, remote sensing and analytic hierarchy process (AHP) technique. *Applied Water Science*. 7, 503–519. https://doi:10.1007/s13201-015-0270-6.

Pourghasemi, H. R., Pradhan, B., Gokceoglu, C., Mohammadi, M., & Moradi, H. R. (2012). Application of weights-of-evidence and certainty factor models and their comparison in landslide susceptibility mapping at Haraz watershed. Iran. *Arabian Journal of Geoscience*. https://doi:10.1007/s12517-012-0532-7

Rahmati, O., Pourghasemi, H. R., & Melesse, A. M. (2016). Application of GIS-based data driven random forest and maximum entropy models for groundwater potential mapping: A case study at Mehran Region, Iran. CATENA, 137, 360–372. https://doi.org/10.1016/J.CATENA.2015.10.010

Razandi, Y., Pourghasemi, H. R., Neisani, N. S., & Rahmati, O. (2015). Application of analytical hierarchy process, frequency ratio, and certainty factor models for groundwater potential mapping using GIS. *Earth Science Information.* 8 (4), 867–883.

Roy, S., Hazra, S., Chanda, A., & Das, S. (2020). Assessment of groundwater potential zones using multi-criteria decision-making technique: a micro-level case study from red and lateritic zone (RLZ) of West Bengal, India. *Sustainable Water Resources Management.* 6 (4), 1-14.

Saaty, T. L. (1980). The Analytic Hierarchy Process: Planning, Priority Setting, Resource Allocation. McGraw-Hill, New York. p 287.

Saha, S. (2017). Groundwater potential mapping using analytical hierarchical process: a study on Md. Bazar Block of Birbhum District, West Bengal. *Spatial Information Research.* https://doi:10.1007/s41324-017-0127-1

Swain, S., Taloor, A. K., Dhal, L., Sahoo, S., & Al-Ansari, N. (2022). Impact of climate change on groundwater hydrology: a comprehensive review and current status of the Indian hydrogeology. *Applied Water Science.* 12:120. https://doi.org/10.1007/s13201-022-01652-0

Tolche, A. D. (2020). Groundwater potential mapping using geospatial techniques: a case study of Dhungeta-Ramis sub-basin, Ethiopia. *Geology, Ecology, and Landscapes.* https://doi.org/10.1080/24749508.2020.1728882

U.S. Geological Survey (2004), Shuttle Radar Topography Mission, 1 Arc Second scene SRTM_u03_n008e004, Unfilled Unfinished 2.0, Global Land Cover Facility, University of Maryland, College Park, Maryland, February 2000.

Wu, W., Lo, M., Wada, Y., Famiglietti, J. S., Reager, J. T., Yeh, P. F., Ducharne, A. & Yang, Z. (2020). Divergent effects of climate change on future groundwater availability in key mid-latitude aquifers. *Nature communications,* 11:3710 https://doi.org/10.1038/s41467-020-17581-y

Yesilnacar EK (2005) The application of computational intelligence to landslide susceptibility mapping in Turkey. Ph.D Thesis Department of Geomatics the University of Melbourne, p 423.

Yifru, B. A., Chung, I., Kim, M., & Chang, S.W. (2021). Assessing the Effect of Land/Use Land Cover and Climate Change on Water Yield and Groundwater Recharge in East African Rift Valley using Integrated Model. *Journal of Hydrology: Regional Studies.* 37, 1-19. https://doi.org/10.1016/j.ejrh.2021.100926